

Force fluctuations in a vertically pushed granular column

E. Kolb^a, T. Mazozi, E. Clément^b, and J. Duran

Laboratoire des Milieux Désordonnés et Hétérogènes^c, Université Pierre et Marie Curie, Boîte 86, 4 Place Jussieu, 75005 Paris, France

Received 5 August 1998 and Received in final form 22 October 1998

Abstract. We present series of experiments on the resistance force encountered by a bottom piston pushing a vertical granular column confined in a two-dimensional cell. We show that, due to the presence of friction at the boundaries and between the grains, the signal shows many complex features. At slow driving velocities, we observe a transition to a stick-slip dynamic instability. Depending on the granular material used, the elementary stick-slip events may either be well characterized or largely distributed. We present a statistical study on the waiting time between events and the distribution of energy release as a function of the spring stiffness and the driving velocity.

PACS. 46.10.+z Mechanics of discrete systems – 05.40.+j Fluctuation phenomena, random processes, and Brownian motion – 83.70.Fn Granular solids

1 Introduction and background

Granular materials form a very complex state of matter which apparent behavior changes drastically with conditions of solicitation (for a recent account on these issues see for example [1,2] and Refs. inside). In a situation of high strains, an analogy is currently made with standard fluid hydrodynamics which is modified to include energy loss due to dissipative collisions [3]. On the other hand, the paradigm to understand the static or the quasi-static behavior of grains is the celebrated Coulomb theory; it is based on the phenomenological laws of solid on solid friction [4,5]. This last notion is strongly backed by some experimental facts. Actually when a granular volume yields, the rupture surface is well defined with an angle that can be related to an internal angle of friction, the analogous of the Coulomb angle for solid friction. The existence of such an angle is also essential to understand why a sand pile may be built with a well defined slope. However this idea is really justified *only* at the yield limit and when other effects like dilatancy are neglected (see for example Refs. [5,6] and Refs. therein).

Recently, some authors have revisited these issues: in the case of static granular assemblies, new constitutive relations were proposed, leading to a set of original predictions for stress distribution [7]. On the other side, the response of a granular assembly to a quasi-static solicitation beyond the yield limit (like a slow shearing or a triaxial deformation test), is not well understood. Practitioners of soil mechanics have developed a framework

where the notion of internal angle is extended to account for macroscopic deformation in the spirit of a plasticity theory [8,9]. As a consequence, new rheological parameters are introduced on a semi-phenomenological basis [5]. But from a fundamental point of view, this approach is not really satisfactory and presently, there is a vivid interest in establishing a deeper understanding of the passage from a description of local granular contacts and force distributions, to a macroscopic description of stress-strain relations [10,11] or alternatively, any other constitutive relations [13]. For example, it is still unclear whether or when, a correct macroscopic description should include fluctuating aspects of the stress, revealing the influence of boundary conditions, material stiffness and/or the possibility of long range stable structures such as vaults [14,15]. Recently, there were several numerical simulations [12,16–19] or experiments [20–25] addressing directly this issue. A problem is still to understand the emergence of a continuous theory since only one of these experiments has shown explicitly that the observed fluctuations, should disappear in the large system limit [23].

There were also several early tests for the validity of a Coulomb theory in the case of a solid interface sliding on a granular assembly [26,35] and also more recent experimental investigations [27–29]. This issue can be viewed from a quite general perspective since the concepts involved span many domains of science from confined molecular systems under shear [30], to the dynamics of solid on solid contact [31], up to the large scales of sliding geological faults [32]. Recently, this experiment was revisited with much scrutiny and in particular, the focus was on precursors of the static yield and on all the dynamical aspects of sliding [29]. A stick-slip dynamical transition was

^a e-mail: kolb@aomc.jussieu.fr

^b e-mail: erc@ccr.jussieu.fr

^c UMR 7603

observed and was shown to depend on the velocity of the driving mechanism which provides a striking analogy with the real behavior of sliding solids [33].

The experimental situation we describe here bears some resemblance with these previous experiments but in a completely different geometry. We report a study on an assembly of grains constrained in a 2D vertical container and pushed vertically through the action of a piston. The piston is connected to a spring which other extremity moves at a constant velocity. We are interested in the dynamics of the forces resisting to pushing. We propose that this resisting motion, which is also very peculiar in view of its dynamical behavior, could be linked to an “arching effect” induced by privileged force paths channeling forces through the granular assembly. The presence of boundaries as well as localized structures in the bulk may introduce large variations in the resistance force, as it was recently reported in the context of an annular cell shearing [21,22] and also of an horizontal wall pushing a granular assembly [23]. In this article we present mostly the relevant phenomenological aspects of the experiment. In particular, we are interested in the process of vault building and in the distribution of elastic energy release during the yield events. Note that a similar situation was studied theoretically in the context of a scalar transport model which also introduces arching effect as a key ingredient for the granular resistance to pushing [34].

2 Experimental setup

The granular material is made of monodisperse steel or aluminium spheres of diameter $a = 1.5$ mm. The use of metallic beads of millimetric size allows to have a good control of geometrical and mechanical properties. The experimental setup is schematically drawn in Figure 1. The beads are placed in a rigid rectangular cell which confines the assembly in a 2-dimensional vertical geometry. The front walls are made of glass and the lateral walls of plexiglass. The distance between the front and back walls is slightly larger than 1.5 mm which optimizes a situation where the frictional resistance of the granular material mostly takes place at the lateral walls. The typical coefficient of friction on plexiglass is about $\mu_w \approx 0.6$ for aluminium beads and $\mu_w \approx 0.5$ for steel beads. The measured coefficient of friction is $\mu = 0.4-0.5$ for oxidized Al beads on an abraded aluminium substrate and $\mu = 0.2$ for steel beads on a substrate of the same material. The width of the cell is $L = 64$ mm, corresponding to a row of 42 beads. The aspect ratio S of the stacking – defined as the ratio of the number of beads in the height to the corresponding number in width – may be varied by adding some horizontal rows. The 2D geometry was chosen for several reasons. First, due to the mono-dispersivity of the beads, the packing is ordered into a very stable triangular lattice and this situation of maximal compacity can easily be reproduced before each experiment. Second, the confined geometry allows a direct visualization of the packing and this information will be of interest when we provide an analysis of the different events.

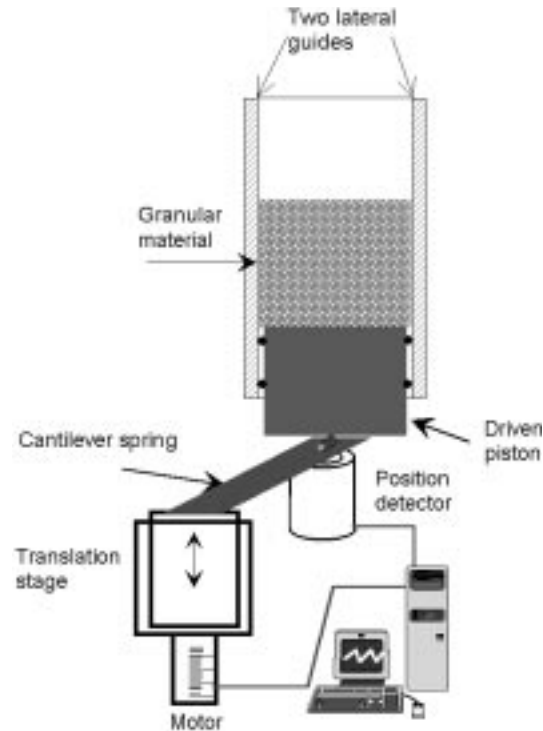


Fig. 1. Experimental setup: the driven piston pushes upward the granular material confined in the 2-dimensional cell. Some inox beads are crimped on each side of the piston in order to reduce friction with boundaries. The granular material is ordered into the triangular lattice and relaxed before each experiment by moving the piston downwards.

The experimental procedure goes as follows: the lowest beads are pushed upwards by a piston which stands on a spring. The spring is mounted on a plateau which is driven at a constant speed V by the translation stage of a stepping motor. The dynamic range of V may be chosen between 0.05 and 50 $\mu\text{m/s}$. The experiment consists in recording the pushing force F when the piston moves upwards. The stiffness of the spring k is varied by using two devices: a set of cantilever springs with different thicknesses or lengths and the beam of an electronic scale. The typical k values for the cantilever springs are between 1000–6000 N/m and for the beam we have, $k = 32285$ N/m. In the first cases the resistance force is deduced from the deflection of the free end of the cantilever spring. This deflection is detected by an inductive displacement sensor. A preliminary set of experiments was performed without bead in the cell in order to determine the level of mechanical and electronic noise of the set “piston + column”.

3 Experimental results and discussion

3.1 General presentation

In a granular material, vertical stresses are transformed *via* contacts between the grains into horizontal stresses

pushing the vertical boundaries. The laws of solid on solid friction tell us that the normal stresses applied to the walls should be transformed into a friction force opposing the vertical motion. Based on this elementary idea, a simple estimate of the yield frictional forces can be done using the heuristic Janssen’s theory [5,35]. This theory introduces a parameter K which transforms any vertical pressure P_v into an horizontal one $P_h = KP_v$. It is clear that this theory is only approximate [5] but *a priori*, it should provide a good estimate of the order of magnitude for the static pressure in a granular column subject to its own weight [25]. In our case, the pushing of the piston produces an upward motion of the beads, which leads to a downward polarization of frictional forces at the lateral walls. By adapting the Janssen’s model to this configuration we derive a qualitative expression of the resistance force of the granular packing to the pushing. The detailed calculations are presented in the appendix. The main result is that the pushing force F , as measured in our experiment, should increase exponentially with the height of the stacking; a value of F can be estimated depending on the friction at the walls. In the framework of this model, it is also possible to estimate the influence of the third dimension stemming from the fact that our experiments are not strictly 2D which could add some supplementary friction. To prevent blocking of the beads inside the cell, we leave a small gap between the glass plates and the beads of approximately: $e \simeq 0.1$ mm. As a consequence, there is a residual transmission of the vertical pressure into an horizontal pressure on the glass walls, *via* the non strictly vertical direction of contacts between the spheres. This effect results in a slightly larger force F^* , dependent on the ratio e/L . In the appendix we also estimate this supplementary friction force.

Now, we report two sets of experiments where the frictional nature of the metallic beads is changed, *i.e.* steel beads where the friction is low and aluminum beads where the friction is high. At this point, it is worth noticing that a friction between the beads is essential to produce resistance to pushing. In fact, if no friction would exist between the beads, nothing would prevent the beads in contact with the edges to roll like in a bead bearing device and therefore, no resistance would be experienced by the piston. It is in fact the frustration of the rotational motion induced by the multi-contacts on the beads which “solidifies” the force network and allows a rigid transmission of forces from the piston to the edges. It is clear that such a feature should intervene somehow in any conceptual representation of the resistance dynamics. This is not obvious from equation (A.3) where all the force network properties are captured into a single effective parameter K . Moreover, due to a certain amount of unavoidable polydispersity (see Ref. [17]) and also to solid friction *between the grains* (see Ref. [19]), we are in a situation where the network of contact forces could be quite disordered, even if the apparent structure of the piling can be viewed as regular. As a consequence, all the dynamical properties of the resistance dynamics experienced by the pushing piston, can *a priori*, come not only from standard solid on

solid dynamical friction laws but also from the complicated force network dynamics which is a signature of the granular aspect of the material.

3.2 Steel beads

The typical response for the set of experiments we performed with steel beads is presented in Figure 2 for parameters: $S = 1.44$, $k = 32285$ N/m and $V = 0.1$ $\mu\text{m/s}$ (Fig. 2a), $V = 1$ $\mu\text{m/s}$ (Fig. 2b) $V = 5$ $\mu\text{m/s}$ (Fig. 2c). From the curves force/distance, we observe, after a fast initial increase of the resisting force, a quasi-plateau or a slowly evolving state. In none of our experiments we can claim that we reached a true steady state. The yield force is always around 2–4 N. It turns out that we empirically observe an increase of the force/distance slope with the amplitude of the driving velocity V . This effect deserves a more systematic study but we leave this for further reports. Direct visualization through the glass walls shows that there is *no reorganization* of the triangular packing and no macroscopic dilation of the stacking. Using the estimation predicted by equation (A.3), we obtain a value of $F = 0.72$ N (after addition of the piston mass $M_p = 32$ g). Use of the modified Janssen’s constant of equation (A.4) would yield: $F^* = 0.73$ N, which is an increase of less than one percent which cannot account for the factor 4 found experimentally. We also checked that a screening length λ with a value half of this one (*e.g.* a value of K twice as large as before) was still unable to provide a correct estimation for the resisting force. The second remark is that the fluctuations around the average resisting forces can be quite different according to the value of the driving velocity. Actually for the stiffness and the aspect ratio mentioned earlier, we evidence a dynamic transition around $V \sim 1$ $\mu\text{m/s}$. Below $V = 0.5$ $\mu\text{m/s}$, we observe a well defined stick-slip regime (see inset Fig. 2a). Note that, for the “stick” part of the dynamics, we tested in several instances that the relations force/displacement correspond to the known spring constants. Nevertheless we did not precisely test for the existence of a possible “creeping” dynamics just before the yield events. This could be interesting but is out of the scope of this article since the time resolution of the data sampling was too large to monitor these effects. Around the value $V \sim 1$ $\mu\text{m/s}$, we observe an intermittent response made of stick-slips and a fluctuating plastic yield (see inset Fig. 2b). Above this velocity, the stick-slip disappears completely and a fluctuating plastic yield response is found (see Fig. 2c). This behavior is reminiscent of general properties of solid on solid friction. For a spring-block system, driven at a constant velocity on a solid substrate, a transition exists from a stick-slip dynamics to a steady-sliding regime. This transition depends on the eigenpulsation of the spring-block system and on the driving velocity V [33]. At low V or low eigenpulsation, a stick-slip appears and occurs periodically with a constant amplitude $\Delta F = F_{max} - F_{min}$. Let us remind that in the simplest solid-on-solid friction model, the static μ_s and the dynamic μ_d coefficients of friction are different ($\mu_s > \mu_d$) and the force drop is $\Delta F = 2(\mu_s - \mu_d)mg$ where mg is

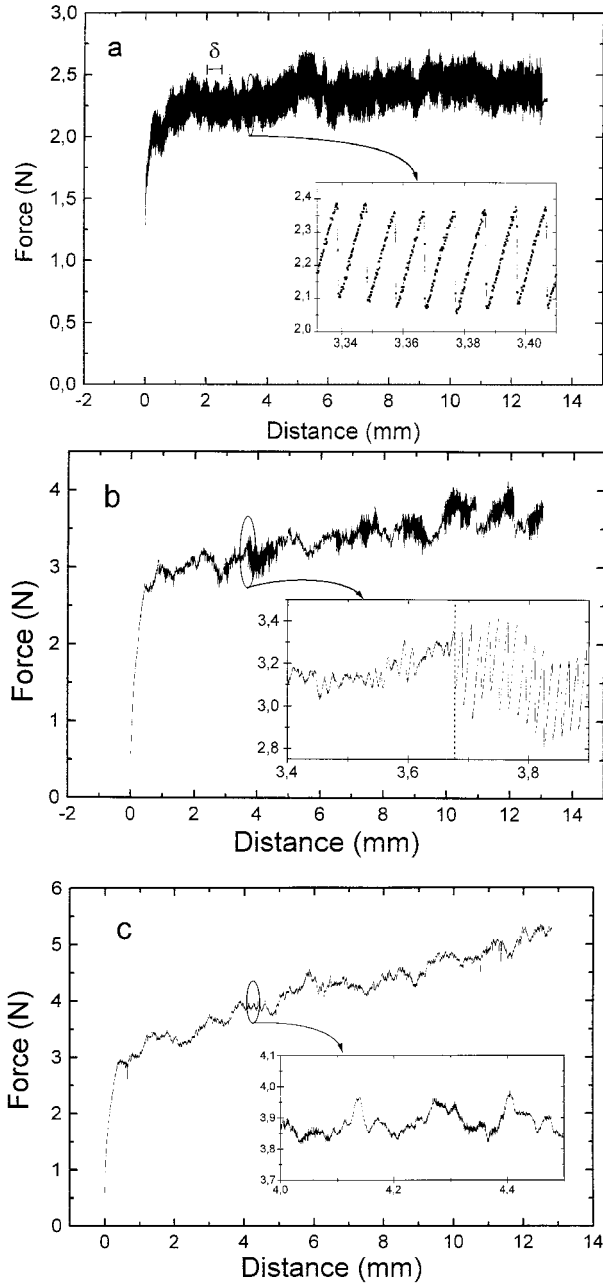


Fig. 2. Fluctuations of the pushing force F as a function of the displacement of the translation stage at the velocity V . The experiments are done with steel beads with $S = 1.44$ and $k = 32285$ N/m. The three figures and their zoom on a reduced distance scale are representative of the different dynamical behaviors. (a) $V = 0.1$ $\mu\text{m/s}$. The force fluctuates around a plateau value. The insert with the saw-teeth signal corresponds to a succession of stick-slip events. This figure is typical of what happens in the stick-slip regime. A modulation of the force on a typical distance scale δ can also be observed. (b) $V = 1$ $\mu\text{m/s}$ marks the transition from (a) to (c). The response is intermittent. At certain times the signal changes abruptly from a well defined stick-slip regime like in (a) to a fluctuating response like in (c) and inversely. (c) $V = 5$ $\mu\text{m/s}$. The fluctuating plastic yield response is characteristic of the high velocity regime.

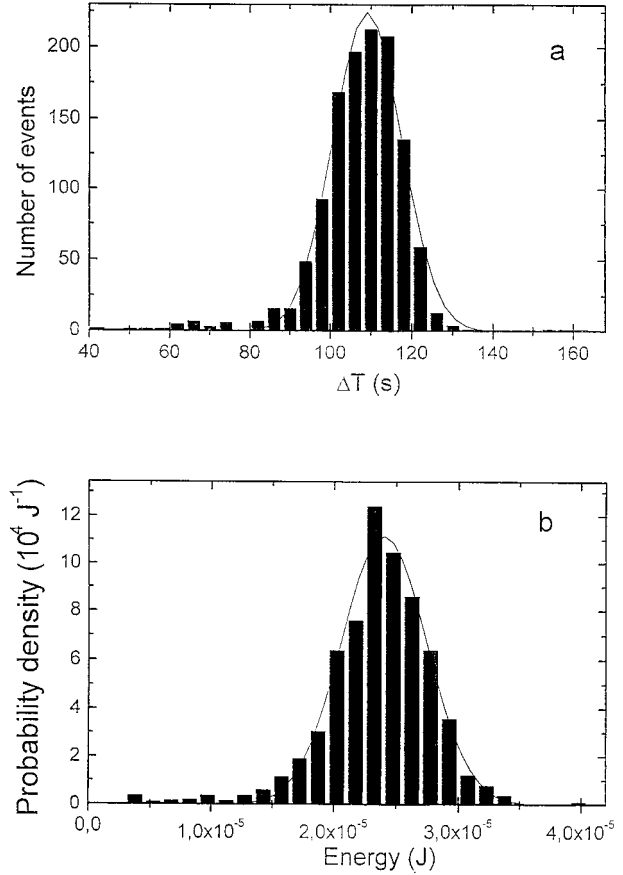


Fig. 3. Distribution of the characteristic parameters of the stick-slip regime in the case of steel beads for $S = 1.44$, $k = 32285$ N/m and $V = 0.1$ $\mu\text{m/s}$. (a) Distribution of the waiting time ΔT between stick-slip events. (b) Probability distribution function of energies ΔE released during the phases of slips. The two distributions are well fitted by Gaussian curves (solid line).

the weight of the solid slider. Now we identify each stick-slip event by detection of the maxima F_{max} just before a slip and the subsequent minimum F_{min} at the beginning of the following stick. Only events corresponding to an amplitude of slip $\Delta F = F_{max} - F_{min}$ larger than a given threshold are stored. We don't take into account fluctuations of the signal which are inside the noise level. After identification of all the events occurring during an experiment, we store for each one F_{max} , F_{min} , the amplitude of the slip ΔF , and the waiting time ΔT . Also, we determine the energy release ΔE of the yield event by calculating:

$$\Delta E = \frac{1}{k} \left[F_{max} \Delta F - \frac{1}{2} (\Delta F)^2 \right]. \quad (1)$$

In opposition to the classical results for solid-on-solid friction on a multi-contact interface, ΔF , ΔE and ΔT do not have constant values but fluctuate around a mean value and their distribution is well fitted by a Gaussian curve (see Figs. 3a and 3b). We also evidence, in some instances, a modulation of the force drop amplitude with a period corresponding to a displacement of the translation stage δ

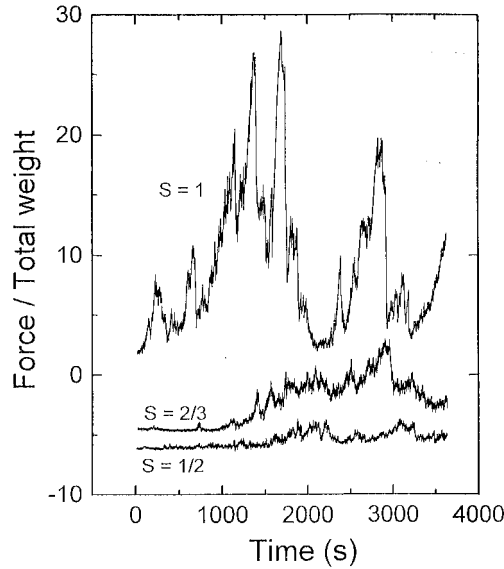


Fig. 4. Fluctuations of the measured force normalized by the total weight of beads and piston as a function of time for different aspect ratios S . From top to bottom: $S = 1$, $S = 2/3$ and $S = 1/2$ for aluminium beads. The three curves are plotted with the same vertical and horizontal scales but for clarity they are vertically shifted (by -4.5 for $S = 2/3$ and by -6 for $S = 1/2$).

of typically a fraction of a bead diameter (see δ in Fig. 2a). We did not observe any systematic variations of δ with the driving velocities. We do not understand the origin of this slow dynamical response but it could correspond to the manifestation of an internal dynamics involving restructuring of the force network in association with the rolling motion of the beads. Note that a modulation was also reported in another experiment on granular friction [29].

3.3 Aluminium beads

Now we describe results obtained for a packing of eroded aluminum beads where the response to vertical pushing is quite different. Importantly, we observed that for Al beads the triangular close packing ordering *is not maintained* through the whole experiment and close to the boundaries, the system experiences some decompaction. In Figure 4 we display three typical signals obtained with different aspect ratios S . The signal is really much more complicated and fluctuating than in the case of steel beads. The force are normalized by the total weight of piston plus beads and the vertical and horizontal scales are the same for the three values of S . It clearly appears that the maximum amplitude of the normalized frictional force is connected to the aspect ratio. The higher is the stacking, the stronger are the resisting forces. This evolution could be *a priori* explained by the exponential increase of the resisting force with the packing height H (see Eq. (A.3)). But, as for steel beads, the quantitative estimation is much smaller than the experimental measurements. For example, the typical forces obtained with an aspect ratio $S = 1$ are between

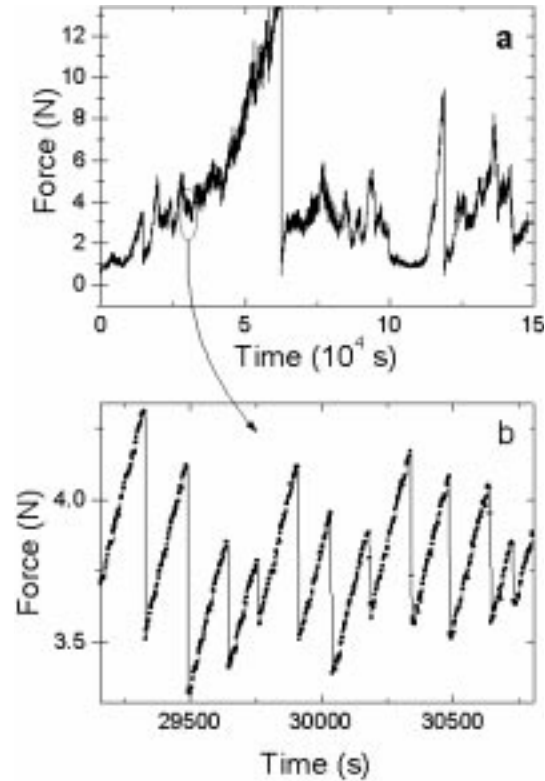


Fig. 5. Fluctuations of the force F as a function of time. The spring stiffness is $k = 5410$ N/m and the velocity of the stepping motor is $V = 0.68$ $\mu\text{m/s}$. (a) the full experiment with the occurrence of big events (b) zoom of the preceding graph showing the small events (stick-slip).

$F = 0.7$ N and $F = 13$ N which is the maximum value of F allowed with our experimental device. Anyway these values are much larger than what equation (A.3) would simply predict ($F = 0.42$ N).

In the following we consider only the case $S = 1$ corresponding to an equal number of aluminium beads along the width and the height of the cell. A typical diagram of the pushing force F as a function of time and a zoom of this signal on a reduced time scale are plotted in Figure 5 for $V = 0.68$ $\mu\text{m/s}$ and $k = 5410$ N/m. We notice that the forces resisting to the vertical pushing have a high level of fluctuation (Fig. 5a) and that the signal is made of series of stick-slip motions of the packing (Fig. 5b). Note that for larger velocities the stick-slip response disappears as for steel beads. These stick-slips are rather disordered. If we observe the signal on a larger time scale, we note a general trend for a slow and progressive increase of the resistance forces. This increasing resistance to pushing is eventually followed by an extremely fast drop of the pushing force characterized by an event of quite large magnitude compared to the typical stick-slip event. By inspection of the granular packing, we noticed that these large force drops are associated with large macroscopic rearrangements taking the form of convection rolls at the lateral walls, apparition of cracks destroying the triangular order or global and important sliding of the packing as a whole. In the course of

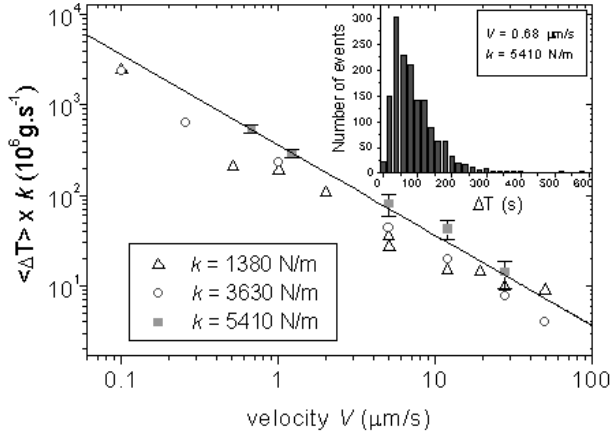


Fig. 6. Log-log plot of the mean duration of a stick-slip event $\langle \Delta T \rangle$ times the spring stiffness k as a function of the stepping motor velocity V . The straight line has a slope of -1 and fits rather well the data obtained for $k = 5410$ N/m. All the points correspond to an aspect ratio of 1. The inset shows the typical distribution of the duration ΔT of the stick-slip events for one particular experiment performed with $k = 5410$ N/m and $V = 0.68$ $\mu\text{m/s}$.

an experiment, we observed only few of such “big events” (about 10 maximum on a total displacement of 100 mm) but a tremendous amount of small stick-slips (typically 1000 in a given experiment). Note that these big events are not observed in the case of steel beads where there is no macroscopic reorganization of the stacking and where the signal of force remains nearly flat.

In the case of aluminium beads, the stick-slip is not periodic and the waiting time between “slip” events ΔT is more distributed than for the steel beads (see inset of Fig. 6). We measured that the mean duration of an event $\langle \Delta T \rangle$, depends on the driving velocity and on the spring stiffness like in the standard stick-slip regime of a solid sliding on a surface. The log-log plot of $k \langle \Delta T \rangle$ versus V clearly shows a tendency for a law of the type: $\langle \Delta T \rangle = \frac{\langle \Delta F^* \rangle}{kV}$ where $\langle \Delta F^* \rangle$ is a typical amplitude of force decrease. For the aspect ratio $S = 1$ the value of $\langle \Delta F^* \rangle$ is 0.360 ± 0.015 N; it corresponds to a constant length scale $\Delta l = \langle \Delta T \rangle V = 66 \pm 3$ μm for a stiffness $k = 5410$ N/m. Note that this force value is not far from the total weight of piston plus beads.

Due to the non-periodicity of the stick-slips, the force release ΔF during an event is expected to be also largely distributed. Unlike solid-on-solid friction the amplitude of ΔF is not at all constant but shows large fluctuations between the “small” and “big” events. Moreover, the amplitudes of slips globally increase with time as the local mean force defined by $F_{mean} = (F_{max} + F_{min})/2$ increases. This effect is illustrated in Figure 7a when we display a zoom on the rising part just before a large yield event. This amplification effect is much more visible and systematic at low velocities ($V = 0.68$ $\mu\text{m/s}$) but also exists for larger velocities as it can be seen in Figure 7b for $V = 5.06$ $\mu\text{m/s}$. On this picture, we observe that after the occurrence of a “big event” (indicated by an arrow in Fig. 7b), the am-

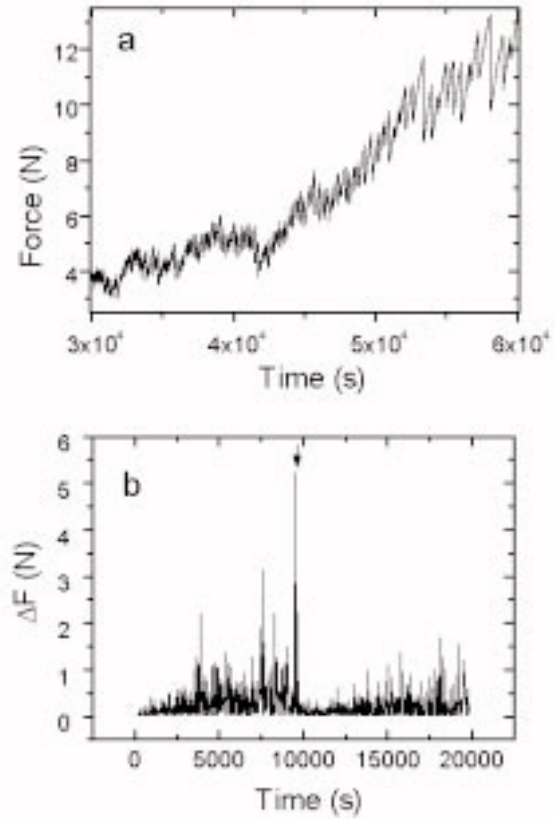


Fig. 7. (a) Evolution of the force with time for $V = 0.68$ $\mu\text{m/s}$ showing the amplification effect: as the mean force increases with time, ΔF also increases. (b) Amplitude of slip ΔF as a function of time for $V = 5.06$ $\mu\text{m/s}$.

plitude of ΔF dramatically drops and reaches about only 1% of the preceding ΔF value. Then after this collapse, the fluctuations are again progressively amplifying with time and the average resisting force increases again. The amplification of ΔF from one stick-slip event to the other seems to be connected to the progressive building-up of a resistant structure over a long time period. This is what we call a vault in the context of this experiment. Inversely, after the occurrence of a big event leading to a global rearrangement of the stacking, the typical force drops ΔF , go to very low values. It seems that there is no more memory of the previous resisting forces in the packing and that strong arches which might have existed in the packing are completely destroyed. It is not clear yet what triggers these “big events” when the resistant force becomes high: it could be some external mechanical vibration or some intrinsic properties defining the maximum resistance of a vault [14,23]. After the occurrence of a big event, the packing slowly reorganizes itself in order to develop increasing resistance to the vertical motion.

Another way of investigating the dynamics of vault building is to look at the energy release ΔE during each event of slip. The statistical distribution of this parameter allows to distinguish clearly the behavior of steel and

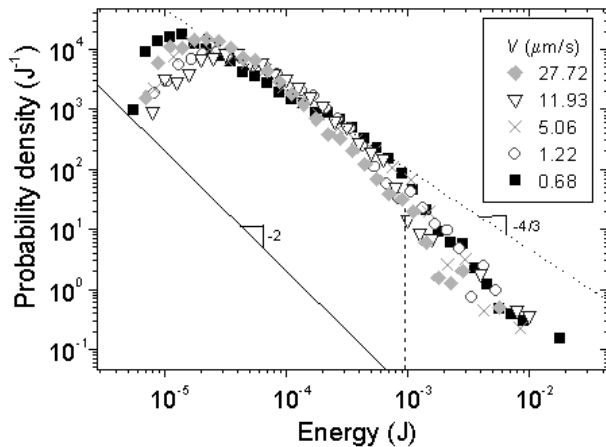


Fig. 8. Probability distribution function of energies ΔE released during the phases of slips for three different stepping motor velocities. The straight line has a slope of -2 and fits the data for small events in the case $V = 27.7 \mu\text{m/s}$.

aluminium beads. The response of the aluminium beads packing is characterized by a very large distribution of energies which span over more than three decades in amplitude. The probability distribution function of ΔE is plotted in Figure 8 on log scales. A power-law regime seems to occur over two decades for the different velocities but it is limited by an upper cutoff around $\Delta E \sim 10^{-3}$ J. Apparently the exponent of the power-law is around $-4/3$ for smaller energy drops and for larger ΔE closer to -2 . This last result should be taken as just indicative due to limited statistics on large ΔE events. Note that large statistical distributions of event sizes were previously found in a model experiment of friction with macroscopic asperities [36]. In this last experiment, the disorder was already present in the distribution of force drops but in our case, this distribution is rather peaked: the disordered response reflects more clearly on the elastic energy distribution, this is a direct consequence of the “vault building” effect.

4 Discussion and concluding remarks

In conclusion, we presented a series of measurements investigating the fluctuating aspects of the resistance force of a granular assembly pushed vertically by a piston and confined in a 2-dimensional cell. The response to this solicitation was studied for two classes of material: steel (low friction) and aluminium (large friction) and for different spring stiffness and driving velocities. In both cases the resisting force is larger than what simple plastic estimation based on a Janssen’s law would predict. At slow pushing velocities the signal is made of elementary stick-slip motions which fluctuate in amplitude but which average properties recall standard solid-on-solid friction laws. On the other hand, fluctuations of the resisting force are quite different for steel and for aluminium beads. In the case of steel beads the pushing force is on an average constant or slowly increasing. At low velocities, we observe the transition to a stick-slip instability characterized by

rather regular features distributed on Gaussian curves. On the other hand, for aluminium beads, the signal is much more complex and fluctuating. At low velocities, the elementary stick-slip events seem to combine to provide a very large resistance to the pushing motion. This resistance can be overcome only *via* major rearrangements of the granular assembly. The small stick-slip events have a large distribution of energy release which takes the form of a power-law distribution with an exponent between -2 and $-4/3$. We interpret qualitatively this phenomenology by the progressive making up of arches which are privileged paths channelling the force exerted by the piston to the boundaries. This effect could provide a mechanical structure very resistant to the pushing motion. The possibility for aluminium beads to create strong arches might be due to a higher coefficient of friction compared with steel beads. We also underlined the possible importance of rotational frustrations but the physical mechanism really involved remains unclear. These preliminary results raise many fundamental questions and call for further investigations. At first, a more complete study is needed to understand how and when the stick-slip regime occurs. Then, a question arises on how these effects would be transported in general 3D situation. Note that these properties may have important practical consequences in many instances where the granular aspect of the matter is essential to control the rheological properties. For example, the industrial problem of the extrusion of dense pastes could be one of these. Finally, the emergence of power-law distributions of elastic energy release in association with friction forces, is an issue deserving more scrutiny by analogy with general geophysical laws characterizing the distribution of seismic events.

We thank Alain Marillier and José Lanuza for their efficient technical assistance. We also acknowledge many discussions with J.P. Bouchaud, P. Claudin, L. Vanel and F. Radjai. We also acknowledge the financial support of the CNRS - PICS program # 563.

Appendix

Janssen’s analysis

The standard analysis of Janssen is based on the division of the packing of beads into homogeneous horizontal slices. It introduces a parameter K which transforms any vertical pressure P_v into an horizontal one $P_h = KP_v$. The calculation is straightforward if one write the equilibrium of an horizontal slice of height dz with a vertical elementary frictional force $dF_r = \varepsilon\mu_w P_h adz = \varepsilon\mu_w KP_v adz$ at one plexiglass wall. This supposes that the friction force is everywhere at the yield limit. The parameter $\varepsilon = \pm 1$ allows a choice in the friction force direction, which can be upwards ($\varepsilon = -1$) or downwards ($\varepsilon = +1$) depending on the direction of motion. Note that we have chosen the positive direction downwards and that the coordinate z

corresponds to the depth in the packing. Thus we obtain:

$$-\frac{dP_v}{dz} + \rho g + \varepsilon 2\mu_w \frac{K}{L} P_v = 0 \quad (\text{A.1})$$

where ρ is the effective density of grains and g is the acceleration of gravity. Note that this first order differential equation only allows for one boundary condition. One usually uses the boundary condition $P_v(0) = 0$ at the top of the stacking in order to predict the pressure for a vertical column at rest. Thereby the usual Janssen's law is recovered for a stacking under its own weight ($\varepsilon = -1$): $P_v(z) = \rho g \lambda (1 - \exp(-\frac{z}{\lambda}))$ (Eq. A.1) where the screening length λ is defined by

$$\lambda = \frac{L}{2K\mu_w}. \quad (\text{A.2})$$

Case of a downward frictional force

In our case the pushing produces an upward motion, then $\varepsilon = 1$. By using the same boundary condition as before, we obtain $P_v(z) = \rho g \lambda (\exp(\frac{z}{\lambda}) - 1)$. This expression holds for a complete downward polarization of the frictional forces at the walls. In this simplified mechanical vision, the pushing force F at a steady-state, is assumed to adjust exactly to compensate the action of gravity combined with the friction at the walls. Therefore, when the granular column yields, the pushing force F is:

$$F = P_v(H)La + M_p g$$

$$F = \rho g \frac{L^2 a}{2K\mu_w} \left(\exp\left(\frac{H}{\lambda}\right) - 1 \right) + M_p g \quad (\text{A.3})$$

where M_p is the piston mass and H is the height of the stacking.

Effect of the third dimension

In this part we attempt to take into account the residual transmission of the vertical pressure into an horizontal pressure on the glass walls due to the small gap e between the beads and the glass plates. We use an argument *à la Janssen* by adding a supplementary term on the left side of equation (A.1): $\varepsilon \mu_{fw} \frac{K^f}{a} P_v$, where μ_{fw} and K^f are respectively, the friction with the frontal glass walls and a Janssen's coefficient in this direction. Therefore, the vertical pushing force has the same structure as in equation (A.3) but with a modified Janssen's coefficient:

$$K^* = K \left(1 + \frac{K^f}{2K} \frac{\mu_{fw}}{\mu_w} \frac{L}{a} \right). \quad (\text{A.4})$$

Estimation of the parameters K and K^f

Now we need an estimation for the Janssen's coefficients. We use the geometrical estimation proposed by Bouchaud

et al. [7] and measured directly by Eloy *et al.* [19] on a regular piling. The angular direction φ of force propagation with respect to the vertical axis, is introduced and we have: $K = \tan^2 \varphi$. Thus we get $K = 1/3$ (with $\varphi = 30^\circ$) and $K^f \simeq (\frac{a}{e})^2$ (with $\varphi \simeq a/e$). Measurements of the bead friction with a glass plate gives $\mu_{fw} \simeq 0.1$, which allows determining the effective parameter K^* and the modified pushing force F^* in every experimental cases we describe in this paper.

References

1. *Friction, Arching and Contact Dynamics*, edited by D.E. Wolf, P. Grassberger (World Scientific, Singapore, 1997).
2. *Powder and Grains 1997, Proceedings of the IIIrd Intern. Conf. on Powder & Grains* edited by R.P. Behringer, J.T. Jenkins (Durham, Balkema, Rotterdam, 1997).
3. J. Jenkins, S. Savage, *J. Fluid Mech.* **130**, 187 (1983); P.Haff, *J. Fluid Mech.* **134**, 401 (1983).
4. C.A. Coulomb, *Mem. Math. Acad. Roy. Sci.* **7**, 343 (1776).
5. R.M. Nedderman, *Statics and kinematics of granular materials* (Cambridge University Press Cambridge, 1992).
6. K.H. Roscoe, *Geotechnique* **20**, 129 (1970); I. Vardoulakis, *Int. J. Numer. Anal. Meth. Geomech.* **4**, 103 (1982); J. Desrue *et al.*, *Geotechnique* **46**, 530 (1996).
7. J.-P. Bouchaud, M.E. Cates, P. Claudin, *J. Phys. I France* **5**, 6389 (1995); S.F. Edwards, C.C. Mounfield, *Physica A* **226**, 1 (1996); J. Wittmer, M.E. Cates, P. Claudin, *J. Phys. I France* **7**, 39 (1997).
8. A. Schoefield, P. Wroth, *Critical State in Soil Mechanics* (McGraw Hill, 1968).
9. J. Fedá, *Mechanics of Particular Materials: The Principles* (Elsevier, 1982).
10. P.A. Cundall, O.D.L. Strack, in *Mechanics of Granular Materials: New Models and Constitutive relations*, edited by M. Satake, J. Jenkins (Elsevier, Amsterdam, 1983), p. 113.
11. J. Goddard, *Continuum Modeling of Granula Assemblies*, in *Physics of Dry Granular Media*, edited by H.J. Herrmann, J.-P. Hovi, S. Luding (Kluwer Academic, Publisher, 1998).
12. J. Goddard, A.K. Didwania, X. Zhuang, *Computer Simulations and Experiment on the Quasi-static Mechanics and Transport Properties of Granular Materials*, in *Mobile Particulate Systems*, edited by E. Guazzeli, L. Oger (Kluwer Academic Publisher, 1995), p. 261.
13. P. Claudin, J.-P. Bouchaud, M.E. Cates, J. Wittmer, *Phys. Rev. E* **57**, 4441 (1998).
14. J. Duran, E. Kolb, L. Vanel, *Phys. Rev. E* **58**, 805 (1998).
15. P. Claudin, J.-P. Bouchaud, *Phys. Rev. Lett* **78**, 231 (1997); M.E. Cates, J. Wittmer, J.-P. Bouchaud, P. Claudin, *Phys. Rev. Lett.* **81**, 1841 (1998).
16. F. Radjai, M. Jean, J.J. Moreau, S. Roux, *Phys. Rev. Lett* **77**, 274 (1996); F. Radjai, D. Wolf, M. Jean, J.J. Moreau, *Phys. Rev. Lett.* **80**, 61 (1998).
17. S. Ouagenouni, J.N. Roux, *Europhys. Lett.* **32**, 449 (1995); S. Ouagenouni, J.N. Roux, *Europhys. Lett.* **39**, 117 (1997).
18. J. Hemmingsson, H.J. Herrmann, S. Roux, *J. Phys. I France* **22**, 291 (1997).
19. C. Eloy, E. Clément, *J. Phys. I France* **7**, 1541 (1997).

20. C.H. Liu, S.R. Nagel, D.A. Schecter, S.N. Coppersmith, S. Majumdar, O. Narayan, T.A. Witten, *Science* **269**, 513 (1995).
21. B. Miller, C. O'Hern, R.P. Behringer, *Phys. Rev. Lett.* **77**, 3110 (1996).
22. D. Howell, R.P. Behringer, in *Powder and Grains 97*, edited by Behringer and Jenkins (Balkema, Rotterdam, 1997), p. 337.
23. A. Ngadi, J. Rajchenbach, *Phys. Rev. Lett.* **80**, 273 (1998).
24. O. Tsoungi, D. Vallet, J.C. Charmet, *Experimental study of the force distributions inside 2D Granular system*, in *Physics of Dry Granular Media* edited by H.J. Herrmann, J.-P. Hovi, S. Luding (Kluwer Acad. Publisher, 1998), p. 149; also *Granular Matter* **1**, 65 (1998).
25. L. Vanel, E. Clément, J. Lanuza, J. Duran, *Pressure Fluctuations in a Granular Column*, in *Physics of Dry Granular Media* edited by H.J. Herrmann, J.-P. Hovi, S. Luding (Kluwer Acad. Publisher, 1998), p. 249; L. Vanel, E. Clément, preprint, 1998.
26. R.L. Brown, J.C. Richards, *Principle of Powder Mechanics* (Pergamon, press, 1970).
27. F. Radjai, P. Evesque, D. Bideau, S. Roux, *Phys. Rev. E* **52**, 5555 (1995).
28. B. Dulieu, F. Radjai, *Interfacial friction in flowing sand*, in *Friction, Arching and Contact Dynamics*, edited by D.E. Wolf, P. Grassberger (World Scientific, Singapore, 1997), p. 281.
29. S. Nasuno, A. Kudrolli, J.P. Gollub, *Phys. Rev. Lett* **79**, 949 (1997); S. Nasuno, A. Kudrolli, A. Bak, J.P. Gollub, to appear in *Phys. Rev. E* (1999); cond-mat 9807018.
30. H. Yoshikawa, P. McGuiggan, J. Israelachvili, *Science* **259**, 1305 (1993).
31. E. Rabinowicz, *Friction and Wear of Materials* (J. Wiley and Sons, New-York, 1965).
32. C.H. Scholz, *The Mechanics of Earthquake and Faulting* (Cambridge University Press, Cambridge, 1990).
33. F. Heslot, T. Baumberger, B. Perrin, B. Caroli, C. Caroli, *Phys. Rev. E* **49**, 4973 (1994).
34. P. Claudin, J.-P. Bouchaud, *Granular Matter* **1**, 71 (1998).
35. H.A. Janssen, *Zeitschr. d. Vereines Deutscher Ingenieure* **39**, 1045–1049 (1895).
36. S. Ciliberto, E. Charlaix, J. Crassoux, C. Laroche, *Experimental study of friction between surfaces with macroscopic asperities*, in *Friction, Arching and Contact Dynamics*, edited by D.E. Wolf, P. Grassberger (World Scientific, Singapore, 1997), p. 61.